THE JOURNAL OF BIOLOGICAL CHEMISTRY VOL. 280, NO. 39, pp. 33516–33524, September 30, 2005

Anillin Is a Substrate of Anaphase-promoting Complex/Cyclosome (APC/C) That Controls Spatial Contractility of Myosin during Late Cytokinesis*[S]

Received for publication, April 28, 2005, and in revised form, July 14, 2005 Published, JBC Papers in Press, July 22, 2005, DOI 10.1074/jbc.M504657200

Wei-meng Zhao[1] **and Guowei Fang**[2]

From the Department of Biological Sciences, Stanford University, Stanford, California 94305-5020

Anillin, an actin-binding protein localized at the cleavage furrow, is required for cytokinesis. Through an *in vitro* expression screen, we identified anillin as a substrate of the anaphase-promoting complex/cyclosome (APC/C), a ubiquitin ligase that controls mitotic progression. We found that the levels of anillin fluctuate in the cell cycle, peaking in mitosis and dropping drastically during mitotic exit. Ubiquitination of anillin required a destruction-box and was mediated by Cdh1, an activator of APC/C. Overexpression of Cdh1 reduced the levels of anillin, whereas inactivation of APC/C^{Cdh1} increased the half-life of anillin. Functionally, anillin was required for the completion of cytokinesis. In anillin knockdown cells, the cleavage furrow ingressed but failed to complete the ingression. At late cytokinesis, the cytosol and DNA in knockdown cells underwent rapid myosin-based oscillatory movement across the furrow. During this movement, RhoA and active myosin were absent from the cleavage furrow, and myosin was redistributed to cortical patches, which powers the random oscillatory movement. We concluded that anillin functions to maintain the localization of active myosin, thereby ensuring the spatial control of concerted contraction during cytokinesis.

Ubiquitin-mediated proteolysis plays key regulatory functions in diverse biological processes, ranging from cell cycle control, cell signaling, transcriptional regulation, immune response, to development. A key ubiquitin ligase in the cell cycle is the anaphase-promoting complex/cyclosome (APC/C),[3] which controls several transitions in the cell cycle (1, 2). APC/C-dependent degradation of cyclin A allows cells to progress from prophase to metaphase, and the degradation of securin by the APC/C triggers the chromosome separation and anaphase onset. Late in anaphase, the destruction of cyclin B1 leads to the inactivation of the Cdk1 kinase activity and exit from mitosis. The APC/C has also been linked to the control of DNA replication, and components of the pre-replication complexes, such as Cdc6 and Cdt1, and an inhibitor of DNA replication, geminin, have all been shown as substrates of the APC/C (3–5).

The activity of the APC/C is tightly regulated in the cell cycle. The APC/C becomes active from prometaphase until the end of G_1. One of the main regulatory mechanisms for the APC/C is through its association with accessory activating factors, Cdc20/fizzy and Cdh1/fizzy-related (6, 7). Both Cdc20 and Cdh1 directly bind to and activate the ligase activity of the APC/C. Cdc20 associates with the APC/C from prometaphase to anaphase, responsible for the degradation of cyclin A, cyclin B, securin, and Kid, whereas Cdh1 maintains the activity of the APC/C from late anaphase through G_1, targeting multiple substrates for degradation (6, 7).

The APC/C recognizes two motifs in substrates: the destruction box (D-box; R*XX*L, where *X* is any amino acid) and the KEN box (8, 9). Although the exact biochemical mechanism for substrate recognition remains to be characterized, it has been reported that APC/C^{Cdc20} recognizes D-box-containing substrates and that APC/C^{Cdh1} recognizes both D-box- and KEN-box-containing substrates (8).

Although the functions of the APC/C in chromosome separation, in mitotic exit, and in coordinating interphase with mitosis are well characterized through identifications of various substrates required for these processes, the potential function of the APC/C in cytokinesis is less clear due to a lack of substrates involved in this process. Physiological studies indicate that cytokinesis is regulated by proteolysis, possibly by the APC/C. For example, the timing of cytokinesis in *Drosophila* has been linked to the degradation of cyclin B and B3 (10). Genetic experiments showed that both cyclin B and cyclin B3 inhibit the initiation of cytokinesis. In mammalian cells, the length of cytokinesis can be extended by the inhibition of the proteasome (11). These observations indicate that proteolysis controls cytokinesis.

To explore a possible link between the APC/C and cytokinesis, we used an *in vitro* expression screen (12) to search for substrates of the APC/C involved in cytokinesis and identified anillin as a substrate of this ligase. Anillin was originally identified as an actin-binding and bundling protein (13) and was later shown to localize at the cleavage furrow during cytokinesis (14). Anillin is required for cytokinesis as injection of an anti-anillin antibody into monkey cells results in binucleated cells (14). In *Drosophila*, RNA interference (RNAi) experiments showed that anillin is required for the completion of cytokinesis at a post-furrowing terminal stage (15, 16). A recent study reports that anillin can bind to non-muscle myosin II *in vitro* (17), although such an interaction has not been reported *in vivo*.

We have reported here that anillin is a substrate of APC/C^{Cdh1}, both *in vitro* and *in vivo*. The levels of anillin fluctuated in the cell cycle, peaking in mitosis, and dropped drastically as cells exited into G_1. At the time when the levels of anillin decreased, Cdh1 became associated with anillin. Indeed, anillin was degraded during mitotic exit in a Cdh1-dependent manner as inactivation of Cdh1, either by RNAi or by overex-

* This work was supported in part by grants from National Institutes of Health (Grant GM062852) and from American Cancer Society (Grant RSG-01-143-01-CCG) (to G. F.). The costs of publication of this article were defrayed in part by the payment of page charges. This article must therefore be hereby marked "*advertisement*" in accordance with 18 U.S.C. Section 1734 solely to indicate this fact.

[S] The on-line version of this article (available at http://www.jbc.org) contains supplemental movies.

[1] Supported by a postdoctoral fellowship from American Heart Association.

[2] To whom correspondence should be addressed: Dept. of Biological Sciences, Stanford University, 337 Campus Dr., MC-5020, Lokey Chemical Biology Bldg., Rm. 137, Stanford, CA 94305-5020.

[3] The abbreviations used are: APC/C, anaphase-promoting complex/cyclosome; RNAi, RNA interference; shRNA, short hairpin RNA; shRNAi, shRNA interference; DIC, differential interference contrast; FACS, fluorescence-activated cell sorter; HA, hemagglutinin; GFP, green fluorescent protein; NMHC II-A, non-muscle myosin II A heavy chain; MRLC, myosin regulatory light chain; p-MRLC, phosphorylated MRLC; MAPK, mitogen-activated protein kinase.

pression of a dominant-negative mutant of Cdh1, stabilized the anillin protein. APC/C^{Cdh1} recognized a D-box in the N-terminal region of anillin, and mutations in this D-box abolished ubiquitination *in vitro* and stabilized the mutant protein *in vivo*. As for the mechanism of anillin function during cytokinesis, we found that anillin is required for concentrating RhoA to the cleavage furrow throughout cytokinesis. In addition, anillin was required for maintaining the active myosin at the cleavage furrow during late cytokinesis. In the absence of anillin, myosin became delocalized to cortical patches, which generated oscillatory movement of cytosol and DNA between the two daughter cells. We concluded that anillin functions to maintain the contractile ring structure at late cytokinesis, ensuring concerted contraction around the cleavage furrow.

EXPERIMENTAL PROCEDURES

In Vitro Ubiquitination Assays—*In vitro* ubiquitination assays were carried out as described previously (7). The ubiquitination reactions were performed at room temperature, analyzed by SDS-PAGE (8–14% gradient gels), and quantified by PhosphorImager (Amersham Biosciences).

To screen for substrates of APC/C, cDNAs from a library enriched in genes expressed in G_2 and mitosis were pooled at 50 cDNAs/pool. Pools of cDNAs were transcribed and translated in rabbit reticulocyte lysates into ^{35}S-labeled proteins, which were then assayed for ubiquitination by APC/C^{Cdh1} (12). Protein pools with putative APC/C substrates were identified by the disappearance of a protein in a Cdh1-dependent manner. Once a positive pool was confirmed, the cDNA pool was subdivided, and a single clone was identified (12). Positive clones were sequenced and analyzed for homology to known sequences.

Plasmids and Antibodies—The coding sequence for full-length anillin was amplified by PCR from human fetal thymus cDNAs (Clontech) and cloned into pCS2+ and pCS2+ FLAG vectors. The deletion mutants of anillin (23–1125 and 45–1125) were generated by PCR. Point mutations were generated using the QuikChange site-directed mutagenesis kit (Stratagene). Full-length Cdh1 was cloned into pCS2+ HA to generate HA-Cdh1, and DNA encoding N-terminal 125 amino acids of Cdh1 were cloned into pCS2+ FLAG to generate FLAG-Cdh1N.

His-tagged anillin amino acids 454–724 and MgcRacGAP amino acids 191–390 were expressed in *Escherichia coli*, purified by nickel-agarose, and used to immunize rabbits for production of antisera. Antibodies were affinity-purified with respective antigens. The specificity of affinity-purified antibodies was confirmed by Western blot analysis and by immunofluorescence staining of wild-type *versus* anillin- or MgcRacGAP knockdown cells (see Fig. 4, *A* and *B*, for the anti-anillin antibody; data not shown for the anti-MgcRacGAP antibody). Anti-CHO1 antibody is a gift from Dr. Ryoko Kuriyama. The following antibodies were from commercial sources: anti-Aurora B (AIM-1) antibody (BD Transduction Laboratories), anti-non-muscle myosin antibody (Biochemical Technology), anti-phospho-myosin light chain 2 (Ser-19) antibody (Cell Signaling), anti-phospho-histone H3 (Ser-10) antibody (Upstate Biotechnology), anti-Cdh1 antibody (Lab Vision), anti-Cdc20, anti-cyclin A, anti-cyclin B1, anti-ECT2, anti-RhoA, anti-p38MAPK, and anti-Hsp70 antibodies (Santa Cruz Biotechnology). Anti-β-tubulin E7 monoclonal antibody was obtained from the Developmental Studies Hybridoma Bank.

Cell Culture and RNAi—HeLa cells and HeLa S3 cells (ATCC) were maintained in Dulbecco's modified Eagle's medium (Cellgro) supplemented with 10% fetal bovine serum and 2 mM L-glutamine (both from Invitrogen). HeLa S3 cells were grown in suspension and synchronized as described previously (7).

RNA interference against Cdh1 was performed as described previously (18, 19). Single-stranded short hairpin RNA (shRNA) was synthesized using the MessageMuter shRNAi production kit (Epicenter) and transfected into HeLa cells using Oligofectamine (Invitrogen). For RNAi of anillin, DNA-based pSUPER constructs (20) were transfected into HeLa cells using Lipofectamine 2000 (Invitrogen). RNAi target sequences are (in the sense orientation): GFP, 5′-GCAAGCTGACCCTGAAGTTC-3′; Cdh1, 5′-GGATTAACGAGAATGAGAAGT-3′, 5′-CAAGCTGCTGGTCTGGAAT-3′; and anillin, 5′-CGCTGTTCTGACAACACTG-3′ and 5′ GGAGAAGAGCCAAGAGGAG3′. For Cdh1 and anillin, two independent siRNA sequences gave similar degree of knockdown and similar phenotypes, confirming the specificity of knockdown.

Immunoprecipitation—Antibodies against anillin were covalently coupled to Affi-Prep protein A beads (Bio-Rad) at a concentration of 0.3 mg/ml. HeLa S3 cells from various cell cycle stages were lysed in Nonidet P-40 lysis buffer (50 mM Tris-HCl, pH 8.0, 140 mM NaCl, 1% Nonidet P-40, 10% glycerol, 0.1 mM EDTA, 1 mM dithiothreitol, 0.5 μM microcystin, 10 μg/ml each of leupeptin, pepstatin, and chymostatin). Lysates were centrifuged, and supernatants were precleared at 4 °C for 1 h with protein A beads that had been coupled with preimmune rabbit IgG. The precleared lysates were then incubated at 4 °C overnight with protein A beads that had been coupled to anti-anillin or Cdh1 antibody. Beads were recovered by centrifugation, washed five times with lysis buffer, and analyzed by immunoblotting with appropriate antibodies.

Immunofluorescence and Time-lapse Video Microscopy—To determine the localization of RhoA, cells growing on glass coverslips were fixed with ice-cold 10% trichloroacetic acid for 15 min (21). For immunofluorescence staining with other antibodies, cells were fixed with 4% paraformaldehyde at room temperature for 15 min. After fixation, cells were permeabilized and blocked with phosphate-buffered saline-BT (1× phosphate-buffered saline, 0.1% Triton X-100, 3% bovine serum albumin) at room temperature for 30 min. Coverslips were subsequently incubated in primary and secondary antibodies diluted in phosphate-buffered saline-BT. Images were acquired with Openlab 4.0.2 (Improvision) under a Zeiss Axiovert 200 M microscope using a ×63 oil immersion lens with a ×1.6 Optovar.

For time-lapse microscopy, HeLa cells stably expressing GFP-Histone H2B were cultured in Leibovitz's L-15 medium (Invitrogen) supplemented with 10% fetal bovine serum (Invitrogen) and 2 mM L-glutamine (Invitrogen). Cells were placed on a microscope stage heated to 37 °C and observed under a differential interference contrast (DIC) and green fluorescence channel on a Zeiss Axiovert 200 M microscope with a ×20 lens plus a ×1.6 Optovar. Images were acquired every 15 s with Openlab 4.0.2 software (Improvision).

RESULTS

Anillin Is a Substrate of the APC/C^{Cdh1} in Vitro—To identify novel substrates of the APC/C involved in cytokinesis, we adapted a small pool expression screen strategy described previously (12) to screen a library of cDNAs enriched in genes transcribed at G_2/M. We used an *in vitro* ubiquitination assay to screen for potential substrates (7) instead of the degradation assay reported previously (5) as the ubiquitination assay is more sensitive than the degradation assay (data not shown). One of the positive clones isolated encoded the N-terminal 496 amino acids of anillin, an actin-binding and bundling protein (Fig. 1*A*) (13). Full-length anillin cDNA was subsequently cloned, and the encoded protein was found to be efficiently ubiquitinated by the APC/C^{Cdh1} (Fig. 1*B*), and to a much lesser extent, by the APC/C^{Cdc20} (data not shown). —The APC/C recognizes the destruction box (D-box) and the KEN box in substrates (8, 9). The first 496 amino acids of anillin contain three puta-

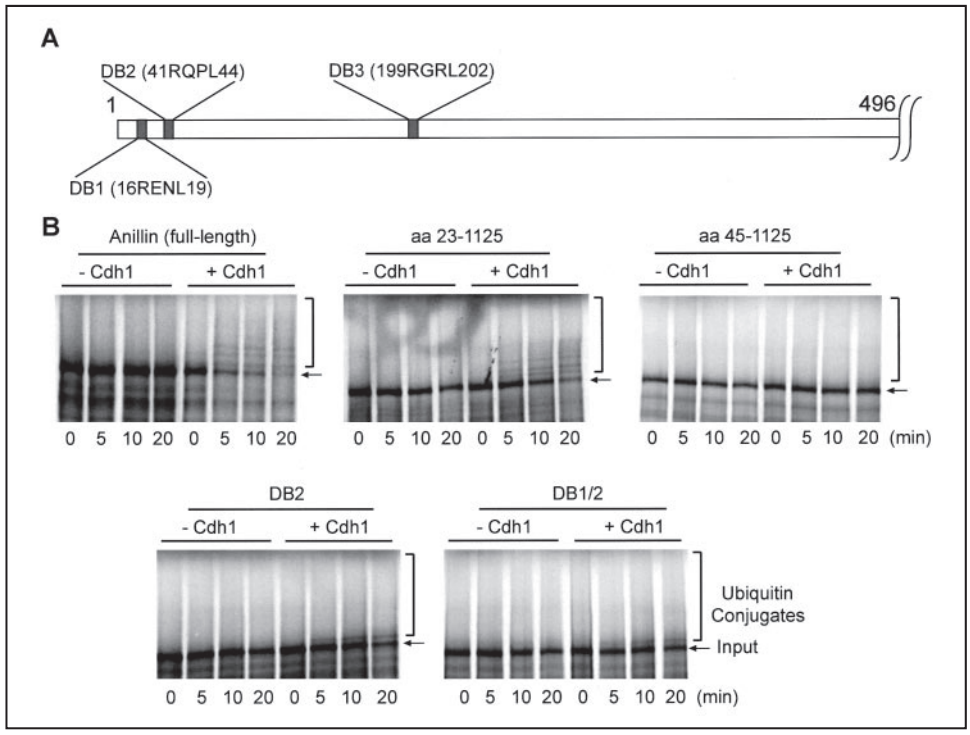

FIGURE 1. **Anillin is specifically ubiquitinated by APC/C^{Cdh1} in vitro.** *A*, a schematic representation of anillin amino acids (*aa*) 1–496 depicting three destruction boxes. *B*, immunopurified APC/C was first incubated with or without recombinant Cdh1 to activate APC/C. ^{35}S-labeled anillin and various mutants were then incubated with APC/C in the presence of ubiquitin-activating enzyme (E1), UbcH10, ubiquitin, and ATP for indicated times. The *arrow* in each panel points to the input substrate, and the *bracket* indicates the position of ubiquitin conjugates. The extent of ubiquitination was judged by the disappearance of the input substrate and by the formation of a ubiquitination ladder migrating slower than the input substrate.

tive D-boxes at amino acids 16–19, 41–44, and 199–202 but no KEN box (Fig. 1*A*). The first two D-boxes are conserved among human, mouse, and *Xenopus* anillin, and the third one is conserved only between human and mouse anillin. Deletion of the first 22 amino acids only partially reduced the ubiquitination efficiency, whereas deletion of the N-terminal 45 amino acids completely abolished the ubiquitination by the APC/C^{Cdh1} (Fig. 1*B*), suggesting that the second D-box is required for the recognition by the APC/C, whereas the first D-box contributes to efficient recognition. Consistent with this, mutation of the second D-box (DB2) (R*XX*L to A*XX*A) in the full-length protein reduced the extent of ubiquitination to only weak mono-ubiquitination, and mutations of the first two D-boxes (DB1/2) reduced the level of ubiquitination to a similar extent (Fig. 1*B*). Thus, the loss of DB2 alone is sufficient to disrupt the recognition by the APC/C.

Anillin Is a Substrate of the APC/C^{Cdh1} in Vivo—To determine whether anillin is a substrate of the APC/C *in vivo*, we first analyzed the levels of the anillin protein in the cell cycle. HeLa S3 cells were synchronized at the G_1/S transition by a double thymidine block, released into fresh media, and harvested every hour after release. The cell cycle profile of released samples was determined by fluorescence-activated cell sorter (FACS), and the time points corresponding to mitosis were identified by the presence of phospho-histone H3 as assayed by Western blot analysis (Fig. 2*A*). Analysis of total cell lysates by Western blotting indicated that the levels of anillin accumulated in S and G_2 phases, peaked in mitosis, and then dropped drastically as cells exited from mitosis into G_1 (Fig. 2*A*). This profile of anillin in the cell cycle is similar to those of known substrates of APC/C such as cyclin B, geminin, and Cdc20 (Fig. 2*A*), suggesting a possibility for an active protein destruction mechanism for anillin during mitotic exit. Kinetic analysis indicated that the degradation of anillin occurred after that of cyclin A (Fig. 2*A*), which happens at prometaphase. To determine the exact cell cycle stage for anillin destruction, HeLa S3 cells were synchronized at prometaphase by a thymidine-nocodazole block and then released into fresh media (Fig. 2*B*). Anillin levels were also down-regulated upon release from prometaphase arrest, and the bulk of anillin was degraded when cells reached late mitosis and exited into G_1. Careful kinetic analysis indicated that the degradation of anillin occurred slightly later than the degradation of cyclin B (Fig. 2*B*). At 1.5 h after release, about 50% of cyclin B was degraded, whereas anillin remained stable at this time point. Biochemical analysis of the fluctuation of anillin in the cell cycle is confirmed at the cellular level. Asynchronous HeLa cells were co-stained with antibodies against cyclin B and anillin. The fluorescence intensity of anillin co-varied with that of cyclin B at individual cell level, high in G_2 and mitotic cells and low in G_1 cells (Fig. 2*C*), indicating that at the cellular level, anillin abundance is regulated in a fashion similar to that of cyclin B, a known substrate of the APC/C.

Next, we analyzed the interaction between anillin and Cdh1. Anillin was immunoprecipitated from cells released from the double thymidine arrest, and the immune complexes were analyzed by blotting with anti-anillin and Cdh1 antibodies. In S, G_2, and early mitotic cells, no association between anillin and Cdh1 was detectable, although Cdh1 in total cell lysates accumulated in G_2 and peaked in mitosis (Fig. 3*A*). Interestingly, Cdh1 associated with anillin in early G_1 when APC/C^{Cdh1} became active, and this association disappeared 3 h after cells exited from mitosis (Fig. 3*A*). The kinetics of the association between anillin and Cdh1 coincided with the kinetics of anillin degradation, suggestive of a role of Cdh1 in the destruction of anillin.

To confirm that the APC/C^{Cdh1} is required for the destruction of anillin, we inhibited the activity of the APC/C^{Cdh1} by RNAi. HeLa cells were transfected with an shRNA targeted against Cdh1 or GFP. Transfection of Cdh1-shRNA, but not GFP-shRNA, reduced the Cdh1 protein levels and resulted in an increase in endogenous anillin and Plk1, a known APC/C substrate (Fig. 3*B*) (7, 22, 23). FACS analysis and quantification of mitotic index indicated that partial knockdown of Cdh1 at the level shown in Fig. 3*B* did not alter the cell cycle profile of transfected cells (data not shown). To demonstrate that this increase is directly due to the stabilization of the anillin protein rather than indirectly through modulating anillin synthesis, we measured the half-life of anillin in knockdown cells. Transfected cells were arrested at prometaphase by nocodazole and then released into fresh media in the presence of cycloheximide, an inhibitor of protein synthesis. In cells transfected with the control shRNA, anillin levels started to decrease 2 h after release. In

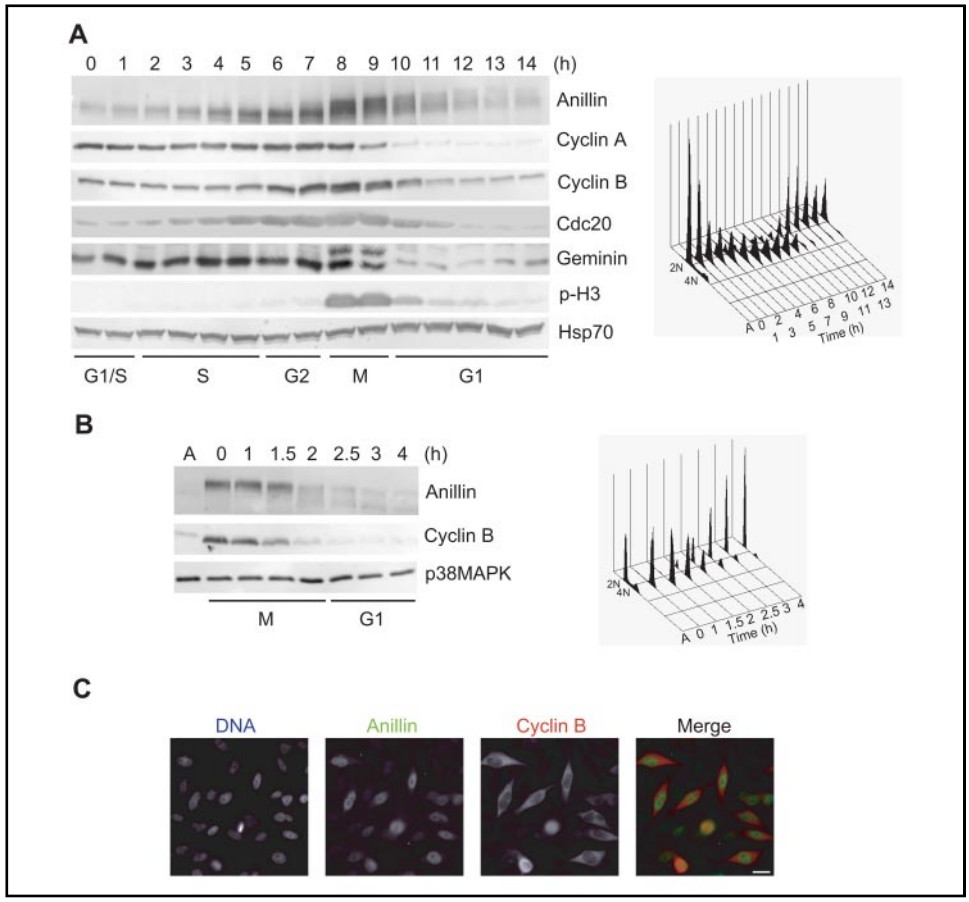

FIGURE 2. **Anillin levels fluctuate during the cell cycle.** *A*, HeLa S3 cells were arrested at G_1/S by a double thymidine arrest and then released into fresh media to allow progression through the cell cycle. The levels of anillin, cyclin A, cyclin B, Cdc20, geminin, phospho-histone H3 (Ser-10) (*p-H3*), and Hsp70 were analyzed by Western blotting of total cell lysates. Cell cycle profile was determined by FACS analysis (*right panel*). *B*, the levels of anillin during mitotic exit. HeLa S3 cells were synchronized at prometaphase by a thymidine-nocodazole arrest and then released into fresh media. The levels of anillin, cyclin B, and p38MAPK were determined by Western blot analysis. *Lane A*, asynchronous cells. *C*, asynchronous HeLa cells were stained with anti-cyclin B and anti-anillin antibodies. DNA was stained with 4′,6-diamidino-2-phenylindole. *Bar*, 20 μm.

contrast, in cells transfected with Cdh1-shRNA, anillin remained at high levels even 4 h after release (Fig. 3*C*). Similarly, Plk1 was also stabilized in Cdh1 knockdown cells. Quantification, by FACS analysis, of the kinetics of mitotic exit upon release from the nocodazole arrest showed that partial knockdown of Cdh1 at the level shown in Fig. 3*C* did not alter the rate of mitotic exit, indicating that the stabilization of anillin in knockdown cells was not due to a delay in transition into G_1.

It has been reported that the amino-terminal 125 amino acids of Cdh1 (Cdh1N) are a dominant-negative mutant for Cdh1 that inhibit the proteolysis of the APC/C^{Cdh1} substrates *in vivo* (24). Thus, HeLa cells were transfected with FLAG-tagged Cdh1N, arrested at prometaphase by nocodazole, and then released into fresh media. In cells transfected with the control vector, the anillin level decreased substantially 2 h after release. In contrast, in cells transfected with FLAG-Cdh1N, anillin remained at high levels at 2 h after release (Fig. 3*D*). Furthermore, anillin remained higher in cells transfected with FLAG-Cdh1N even at 4 and 5 h after release. FACS analysis indicated that control- and FLAG-Cdh1N-transfected cells had similar cell cycle profiles at 4 and 5 h after release (Fig. 3*D*). In addition, cyclin B levels were stabilized upon the overexpression of Cdh1N, consistent with the inhibition of the APC/C^{Cdh1} by Cdh1N.

Since the second D-box at the N-terminal region is required for *in vitro* ubiquitination of anillin by the APC/C^{Cdh1} (Fig. 1*B*), we determined whether this D-box is recognized during the degradation of anillin *in vivo*. FLAG-tagged wild-type or DB2 anillin were co-transfected with a vector or HA-Cdh1 into HeLa cells. Overexpression of Cdh1, which hyper-activated the APC/C^{Cdh1}, reduced the levels of wild-type anillin (Fig. 3*E*), confirming the degradation of anillin by the APC/C pathway *in vivo*. Interestingly, overexpression of Cdh1 did not affect the level of anillin DB2. Overexpression of DB1/2 anillin gave similar results (Fig. 3*E*). Thus, DB2 was necessary for the degradation of anillin *in vivo*, consistent with the *in vitro* ubiquitination results (Fig. 1*B*). FACS analysis indicated that overexpression of Cdh1 reduced the G_2/M and S population (Fig. 3*E*), likely due to the inhibition of the cyclin A accumulation at the G_1/S transition. However, co-expression of the three anillin constructs with Cdh1 gave very similar cell cycle profiles, indicating that the stabilization of the D-box mutants were not due to a change in the cell cycle states.

Anillin Controls Spatial Contractility during Late Cytokinesis—We next analyzed the function of anillin during cytokinesis. Given that anillin is localized to the presumptive cleavage furrow at anaphase, we investigated whether anillin acts to trigger initiation of cytokinesis or is only required for the progression or completion of cytokinesis. HeLa cells were transfected with pSUPER-anillin, which expressed an shRNA-targeting anillin transcript. At 24 h after transfection, the levels of anillin were reduced by at least 80% in pSUPER-anillin transfected cells (Fig. 4*A*). The efficiency of knockdown increased over time and lasted up to 96 h after transfection. When analyzed by immunofluorescence antibody staining, anillin was localized at the contractile ring in control-transfected cells undergoing anaphase B and cytokinesis (Fig. 4*B*), consistent with an earlier report (14). In pSUPER-anillin transfected cells (~80% transfection efficiency), anillin was absent from the cleavage furrow in 80% of randomly selected cells undergoing anaphase B and early cytokinesis ($n = 35$) (Fig. 4*B*), indicating an efficient knockdown at the cellular level.

Anillin is required for cytokinesis; at 36 h after transfection, 43% of knockdown cells were binucleated, whereas less than 4% cells were binucleated in control transfection, consistent with a previous report (14). To characterize the nature of the defect, transfected cells were imaged in time-lapse images under DIC starting from 30 h after trans-

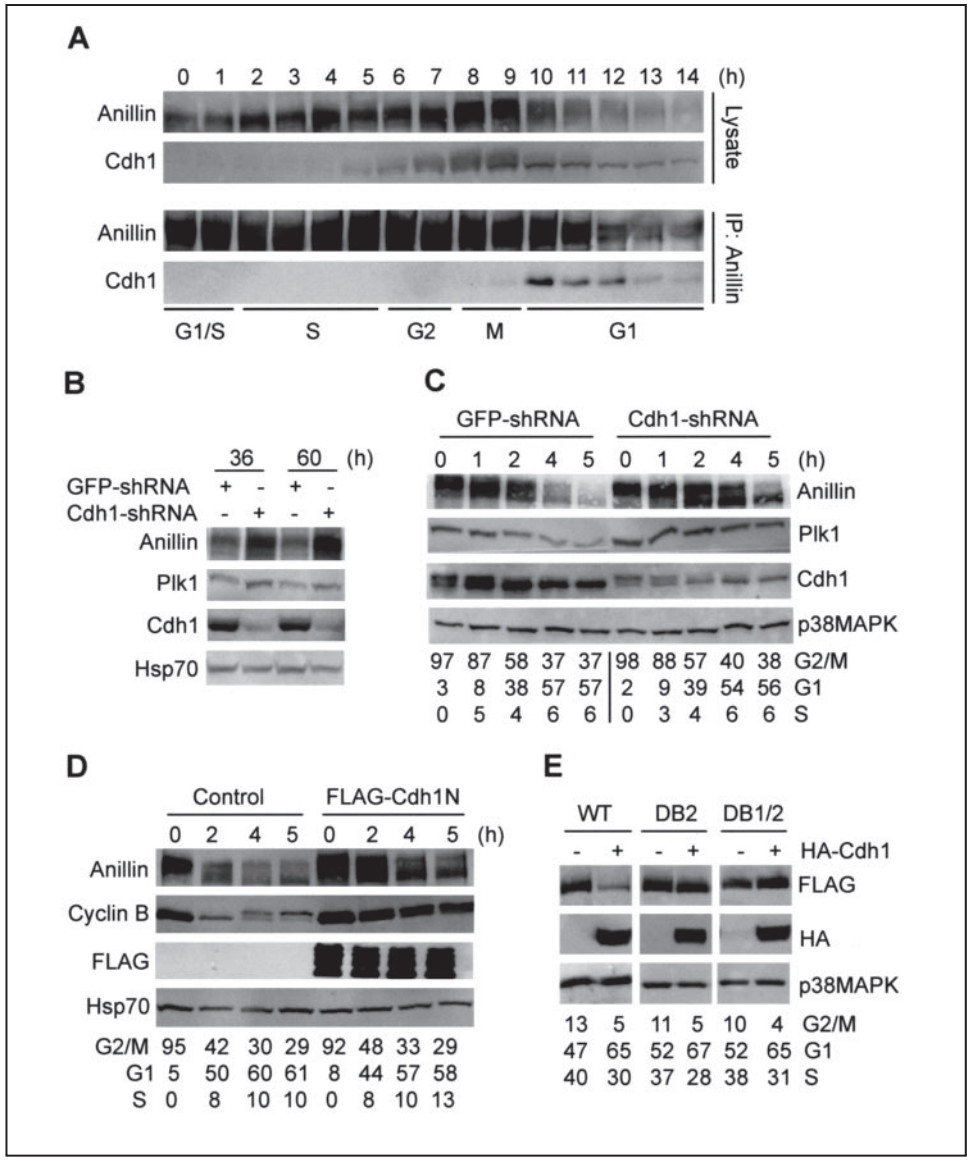

FIGURE 3. **Anillin is degraded in a Cdh1-dependent manner *in vivo*.** *A*, association between anillin and Cdh1. HeLa S3 cells were released from a double thymidine block for the times indicated. Lysates of synchronized HeLa S3 cells were immunoprecipitated (*IP*) with an anti-anillin antibody and followed by immunoblotting. *B*, HeLa cells were transfected with GFP- or Cdh1-shRNAs and harvested at the indicated times after transfection. The levels of anillin, Plk1, Cdh1, and p38MAPK were determined by Western blot analysis of total cell lysates. *C*, HeLa cells were transfected with GFP- or Cdh1-shRNAs and arrested at prometaphase by incubating with nocodazole for 20 h. Cells were then released into fresh medium in the presence of 10 μg/ml cycloheximide and harvested at the indicated times after release. The levels of anillin, Plk1, Cdh1, and p38MAPK were determined by Western blot analysis. *D*, HeLa cells were transfected with FLAG or FLAG-Cdh1N and arrested at prometaphase by incubating with nocodazole for 20 h. Cells were then released into fresh media and harvested at the indicated times after release. The levels of anillin, FLAG-Cdh1N, cyclin B, and Hsp70 were determined by Western blot analysis. The kinetics of mitotic exit was monitored by FACS analysis and showed as a percentage of cells at each cell cycle stage for the release time points (*C* and *D*). *E*, FLAG-anillin, FLAG-anillin DB2, or FLAG-anillin DB1/2 was transfected into HeLa cells with HA or HA-Cdh1. The levels of FLAG-anillin, HA-Cdh1, and p38MAKP were determined by Western blot analysis. Cell cycle profile was determined by FACS analysis. *WT*, wild type.

fection. Although cells transfected with pSUPER initiated and progressed through cytokinesis with normal kinetics (Fig. 4*C*, and see Supplemental Materials, Movie 1), 21 out of 25 randomly recorded cells that had been transfected with pSUPER-anillin displayed a cytokinesis defect and generated binucleation (Fig. 4*D*, and see Supplemental Materials, Movie 2). In cells depleted of anillin, anaphase and the initiation of cytokinesis were normal. When the cleavage furrow ingressed to about 40% of the cell diameter, the furrow was held at this constant size for about 10 min before the furrow eventually regressed (Fig. 4*D*, *red arrow*). Interestingly, during this 10-min window, the cytosol and DNA of the two daughter cells rapidly moved back and forth across the cleavage furrow, similar to an independent observation published during the preparation of this report (17). This phenotype was confirmed by a second knockdown construct and therefore is specific to the loss of anillin function (data not shown). Thus, anillin was required for the completion of furrow ingression.

The oscillatory movement observed in anillin knockdown cells suggested that anillin is involved in regulating the intracellular contractility. Thus, understanding the molecular basis of this oscillatory movement will provide insights on the cellular function of anillin. This movement could be powered either by microtubule-associated kinesins or by the actin-based myosin motor. To differentiate these two possibilities, we used chemical inhibitors specific to microtubules and to actin cytoskeleton. Cells with anillin knockdown were imaged during anaphase and cytokinesis by time lapse images. As soon as the oscillatory movement was initiated, chemical inhibitors were added to the culture media, and the progression of cytokinesis followed. The addition of nocodazole, a microtubule-depolymerizing drug, did not interfere with the oscillatory movement (Fig. 5*A*, and see Supplemental Materials, Movie 3). Control experiments showed that the concentration of nocodazole used (8 μM) here was sufficient to depolymerize microtubules *in vivo* (data not shown). Thus, microtubule-based kinesin motor activities are unlikely responsible for this oscillatory movement. On the other hand, the addition of cytochalasin B, an inhibitor of actin polymerization, led to an immediate cessation of the oscillation, indicating that this movement is actin-based (Fig. 5*B*, and see Supplemental Materials, Movie 4). Consistent with this, the addition of blebbistatin, a specific inhibitor of nonmuscle myosin II (11), also abolished the movement between the two daughter cells (Fig. 5*C*, and see Supplemental Materials, Movie 5). We concluded that in anillin knockdown cells, myosin is activated, but the motor activity is misregulated spatially.

Anillin Is Required for the Localization of the Cleavage Furrow Components during Late Cytokinesis—We investigated the localization of several cleavage furrow components in anillin knockdown cells. Non-

muscle myosin II A heavy chain, NMHC II-A, is a component of the actomyosin ring and was concentrated at the cleavage furrow throughout cytokinesis (Fig. 6*A*) (11, 25). In anillin knockdown cells, NMHC II-A localized to the cleavage furrow during early cytokinesis when the furrow ingressed normally (Fig. 6*A*). However, NMHC II-A was absent from the furrow during late cytokinesis and was mislocalized to the cortical regions during the oscillatory movement (Fig. 6*A*), consistent with the observed random cortical contraction and the lack of furrow ingression.

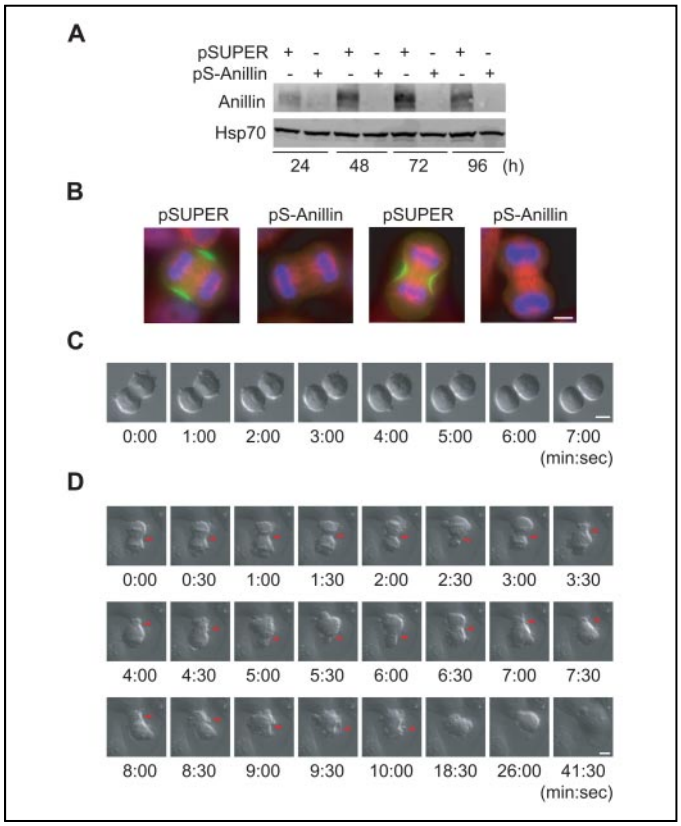

FIGURE 4. **Anillin is required for the completion of cytokinesis.** *A*, immunoblot analysis of anillin knockdown cells. HeLa cells were transfected with pSUPER or pSUPER-anillin (*pS-Anillin*) and harvested at the times indicated. The levels of anillin and Hsp70 were determined by Western blot analysis of total cell lysates. *B*, cells transfected with pSUPER or pSUPER-anillin were stained for anillin (*green*), β-tubulin (*red*), and DNA (*blue*). Merged images are shown. *Bar*, 5 μm. *C* and *D*, selected frames from time-lapse movies of HeLa cells transfected with either pSUPER (*panel C* and Movie 1) or pSUPER-anillin (*panel D* and Movie 2). Cells were imaged every 15 s starting from 30 h after transfection, and images of DIC are shown. *Bar*, 10 μm.

We next examined the activity state of the myosin motor in anillin knockdown cells. The myosin regulatory light chain (MRLC) is phosphorylated on threonine 18 and serine 19, and the phosphorylation is required for the myosin II motor activity (26, 27). Staining with an antibody specific to MRLC phosphorylated at Ser-19 (p-MRLC) revealed that p-MRLC localized to both the cleavage furrow and the central spindle throughout cytokinesis in control-transfected cells (Fig. 6*B*). In anillin knockdown cells, the localization of p-MRLC was normal during early cytokinesis but defective during late cytokinesis when the oscillatory movement occurred.

During cytokinesis, the phosphorylation of MRLC is controlled by the small GTPase RhoA, which itself also localizes to the cleavage furrow from late anaphase through cytokinesis (28, 29). Staining with an anti-RhoA antibody revealed that the RhoA signal at the cleavage furrow was reduced by 80% in anillin knockdown cells ($n = 23$) (Fig. 6*C*). In contrast to NMHC II-A and p-MRLC, the reduction of RhoA signal at the cleavage furrow occurred from early cytokinesis, at a time when the furrow ingression appeared normal, and the low The levels of RhoA signal were maintained throughout cytokinesis. Thus, anillin contributed to the efficient accumulation of RhoA at the cleavage furrow.

Assembly of the Central Spindle Is Independent of Anillin—The central spindle plays an important role in the initiation and completion of cytokinesis (30). To determine whether anillin controls the central spindle structure, we examined the localization of MgcRacGAP, MKLP1, ECT2, and Aurora B kinase, all of which localize to the spindle midzone during cytokinesis (Fig. 7) and are required for cytokinesis (31–35). In anillin knockdown cells, the localization of these proteins was not affected (Fig. 7). The central spindle structure was normal at early cytokinesis and persisted during the oscillatory movement (Fig. 7, *A* and *C*). Therefore, a loss of anillin does not affect the central spindle structure.

DISCUSSION

APC/C is a key ubiquitin ligase that controls sister chromatid separation, mitotic exit, and G_1/S transition (1, 2). We have identified anillin, a component of the cleavage furrow, as a substrate of APC/C, suggesting a possible role of APC/C in cytokinesis. Although anillin is not required for the initial assembly of the cleavage furrow structure, it is required for the maintenance of the cleavage furrow structure and for the completion of furrow ingression. In the absence of anillin, the accumulation of RhoA at the cleavage furrow was impaired. At early cytokinesis, the assembly of myosin II subunits to the contractile ring was not affected, and the furrow ingression occurred normally in anillin knockdown cells. However, at late cytokinesis, the furrow ingression failed to complete, and the cytosol and DNA from two daughter cells rapidly moved back

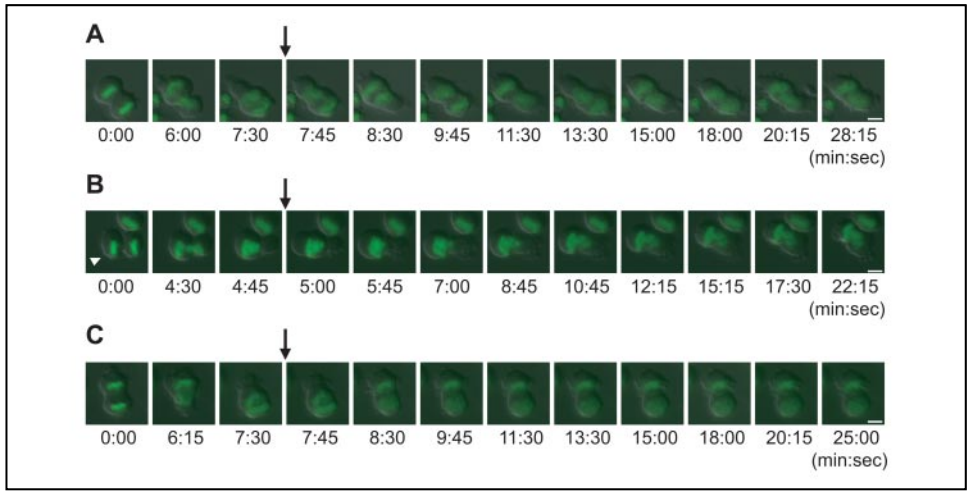

FIGURE 5. **Anillin controls the contractility of the actomyosin ring.** Selected frames from time-lapse movies of HeLa cells stably expressing GFP-histone H2B are shown. Cells were transfected with pSUPER-anillin and imaged every 15 s starting from 30 h after transfection. Nocodazole (8 μM) (*A*), cytochalasin (13 μM) B (*B*), and blebbistatin (50 μM) (*C*) were added (at the times indicated by the *arrows*) as soon as the oscillatory movement began. Both DIC and green fluorescence images were recorded, and merged images are shown. The *arrowhead* in *panel B* points to the cell undergoing cytokinesis. *Bar*, 10 μm.

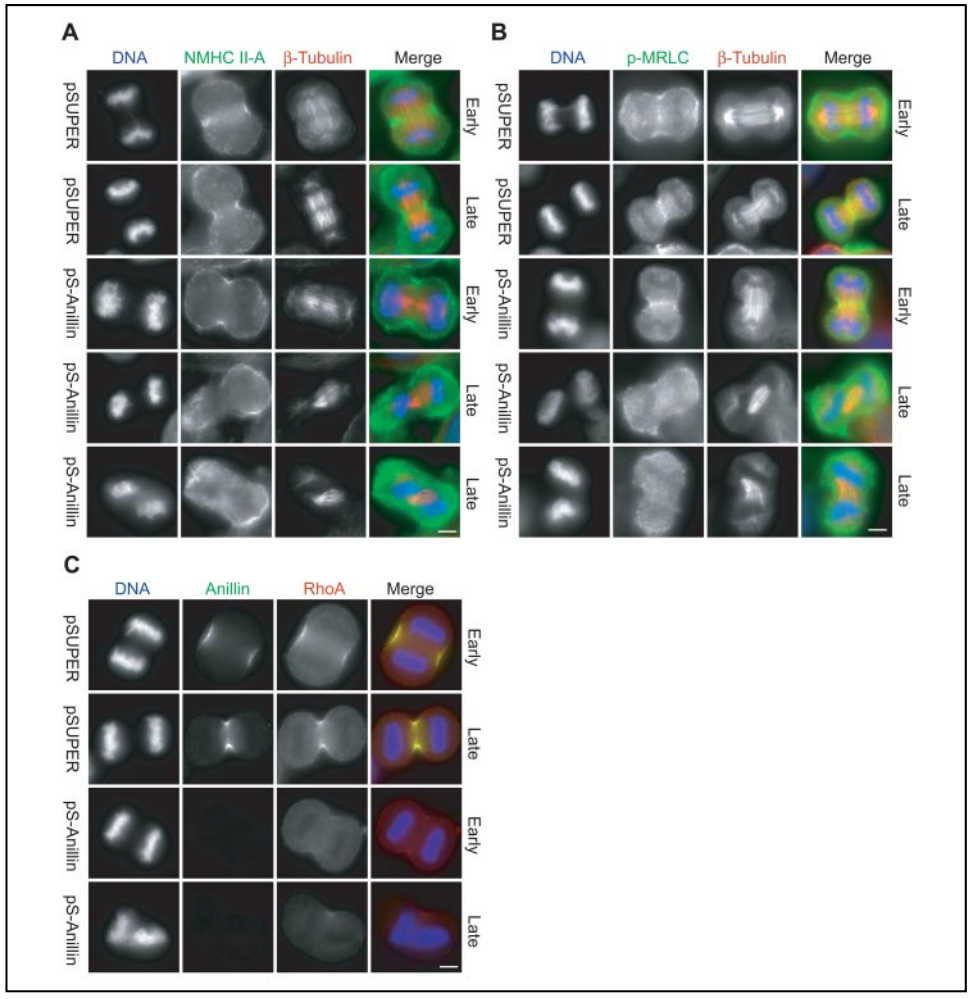

FIGURE 6. **Anillin is required for the localization of the cleavage furrow components.** *A–C*, cells were transfected with pSUPER and pSUPER-anillin (*pS-anillin*) and immunostained for the indicated antigens. The color of the antigen is labeled in each panel. *Early* and *Late* represent cells in early and late cytokinesis, respectively. *Bar*, 5 μm.

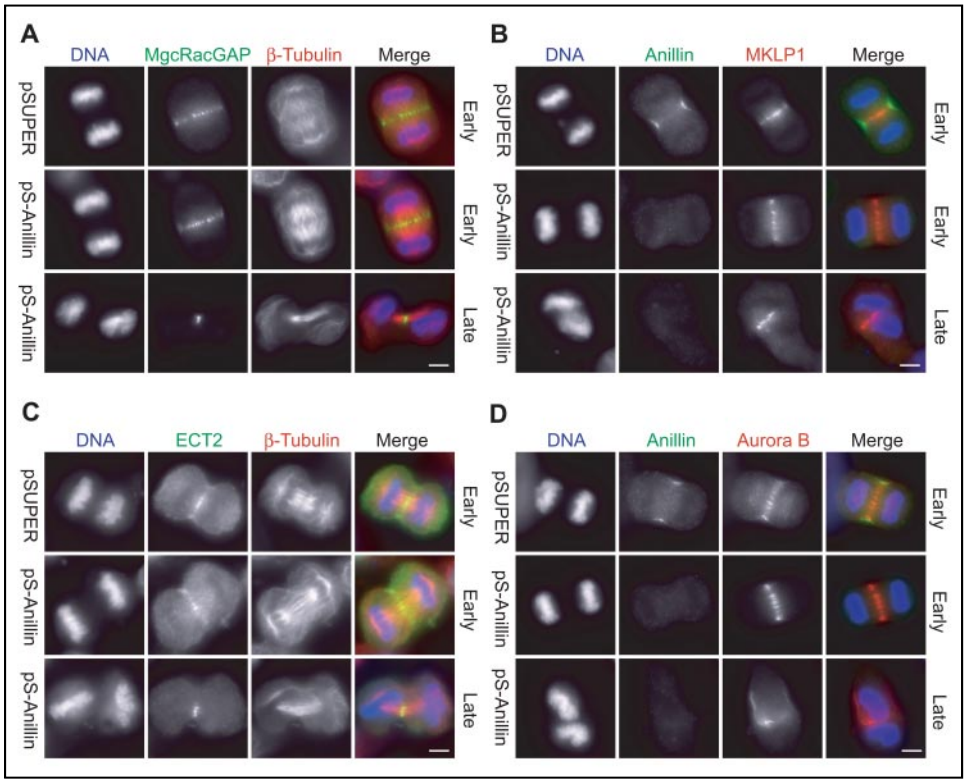

FIGURE 7. **Anillin is not required for the localization of the spindle midzone components.** *A–D*, cells were transfected with pSUPER or pSUPER-anillin (*pS-anillin*) and immunostained for the indicated antigens. The color of the antigen is labeled in each panel. *Early* and *Late* represent cells in early and late cytokinesis, respectively. *Bar*, 5 μm.

and forth across the cleavage furrow, whereas the size of the furrow was held constant. During this movement, both myosin II heavy chain and the active p-MRLC were redistributed from the cleavage furrow to cortical patches. In fact, this oscillatory movement was powered by the mislocalized active myosin as the addition of blebbistatin led to an immediate cessation of the movement. We concluded that anillin functions to maintain the localization of active myosin at the cleavage furrow, thereby ensuring the spatial control of concerted contraction during cytokinesis.

Anillin Is a Substrate of APC/C—The following evidence indicates that anillin is a physiological substrate of the APC/C. First, the full-length anillin is efficiently ubiquitinated by APC/C^{Cdh1} *in vitro* (Fig. 1). Second, both Western blotting and immunofluorescence experiments showed that, similar to cyclin B, the levels of anillin fluctuate in the cell cycle, peaking in mitosis and dropping drastically as cells exit into G_1 (Fig. 2). Third, anillin directly associates with Cdh1 during mitotic exit *in vivo*, at a time when anillin is rapidly degraded (Fig. 3). Fourth, knockdown of Cdh1 or overexpression of the dominant-negative form of Cdh1 leads to an increase in anillin, and this increase is directly due to the stabilization of the anillin protein during mitotic exit (Fig. 3). Fifth, overexpression of Cdh1 results in a decrease in wild-type anillin levels (Fig. 3). Finally, APC/C specifically recognizes a D-box in the N-terminal region of anillin, and mutations of this D-box prevent ubiquitination *in vitro* and lead to stabilization of the mutant protein *in vivo* (Figs. 1 and 3).

What is the physiological role of anillin degradation? Cytokinesis requires active protein degradation through the ubiquitin-dependent pathway as the length of cytokinesis can be extended by inhibition of the proteasome activity (11). Although the exact substrates responsible for this lengthening of cytokinesis are not known, anillin may provide a possible link between proteolysis and cytokinesis. In fact, a fission yeast anillin-like protein, Mid2p, is also degraded by the ubiquitin-dependent pathway, albeit mediated by the Skp1/Cdc53/F-box (SCF) ligase (36). It has been proposed that timely destruction of Mid2p is linked to the disassembly of septin rings at the end of each cell cycle, which may be important for normal cell cycle progression (36). Although destruction of anillin may serve a similar function in mammalian cells, we found that partial knockdown of Cdh1 stabilizes anillin without affecting the kinetics of mitotic exit and cytokinesis (Fig. 3*C*), suggesting that degradation of anillin is not an essential mechanism for control of cytokinesis.

Beyond cytokinesis, the degradation of anillin may be important for cell physiology in G_1. Actin has been proposed to have multiple functions in the nucleus of interphase cells, ranging from chromatin remodeling to RNA transcription and transport and the organization of nucleoskeleton (37). Interestingly, when ectopically expressed, anillin is sequestered in the nucleus in interphase cells. As an actin-binding and bundling protein, untimely accumulation of anillin in G_1 and S phase cells may interfere with the nuclear function of actin. Thus, the degradation of anillin at early G_1 by the APC/C provides a mechanism for the clearance of anillin in interphase cells. Indeed, we found that expression of anillin, even the wild-type protein at a low level, is extremely toxic to the cells and leads to massive cell death (data not shown), underscoring the importance of tight regulation of the anillin levels in the cell cycle. We propose that APC/C-dependent proteolysis is an intrinsic mechanism for this regulation. However, despite our extensive efforts in controlling the levels of transfected anillin, we were not able to alleviate the high toxicity of ectopically expressed wild-type anillin (data not shown). Thus, we were not able to test the physiological consequence of expressing a non-degradable anillin mutant.

Anillin Controls Concerted Contraction at the Cleavage Furrow—We have reported here that anillin is required for the proper localization of myosin II and RhoA to the cleavage furrow. The timing of these requirements is different between RhoA and myosin. The effect on the localization of myosin and only detectable at late cytokinesis. In the absence of anillin, the localization of myosin II subunits was not affected during early cytokinesis, and myosin only became delocalized at late cytokinesis. However, anillin is required to concentrate RhoA to the cleavage furrow starting from anaphase B. Anillin may maintain the RhoA localization through direct association since we observed a weak interaction between anillin and RhoA in our *in vitro* direct binding assay (data not shown). Thus, although anillin knockdown cells failed cytokinesis at a late stage, our results indicated that the contractile ring structure was defective at the molecular level long before any morphological defects became observable.

Why does cytokinesis only fail at a late stage in anillin knockdown cells? Although we cannot exclude the possibility that this late phenotype is due to an incomplete knockdown by RNAi, this is unlikely since the knockdown efficiency reached greater than 90% by the time of our analysis (at 36 h after transfection; Fig. 4; data not shown) and since injection of an anti-anillin antibody gave a similar late phenotype (14).

Cytokinesis fails at a time when myosin becomes delocalized from the cleavage furrow, although the causal relationship between these two remains to be established. Biochemically, it has been reported that anillin binds to myosin II *in vitro* (17), but no association between myosin and anillin was detectable in anaphase cells or in cells undergoing cytokinesis (data not shown). In addition, myosin is localized to the cleavage furrow normally during anaphase and early cytokinesis in the absence of anillin, indicating that a direct interaction between anillin and myosin is not required for targeting myosin to the cleavage furrow, at least during early cytokinesis.

We propose two possible models, which are not mutually exclusive, to explain the failure in completing cytokinesis in anillin knockdown cells. First, a lack of the RhoA concentration at the cleavage furrow may lead to the incomplete furrow ingression since RhoA is the crucial upstream activator for the phosphorylation of MRLC (30). A recent fluorescence resonance energy transfer study showed that in HeLa cells, the levels of RhoA-GTP decrease rapidly upon entry into mitosis, reach the lowest at anaphase, and then increase gradually during cytokinesis (38), suggesting that the requirement for the RhoA activity may increase as cytokinesis progresses. Thus, the residual RhoA protein at the cleavage furrow may be sufficient for the initial ingression of the cleavage furrow in anillin knockdown cells but is not sufficient for the completion of the furrow ingression.

Alternatively, the lack of myosin at the cleavage furrow during late cytokinesis may simply result from a defect in the mechanical structure of the furrow. The contractile ring has to be able to maintain the structural integrity to withstand the mechanical force exerted on the cleavage furrow. On the other hand, the contractile ring is not a static structure but has to undergo constant remodeling (through actin polymerization and depolymerization) during furrow ingression. Thus, the actomyosin ring at the furrow is expected to be dynamic and yet stable, and anillin, an actin-binding and bundling protein, may be important for maintaining this dynamic stability of the actomyosin contractile ring structure. The effect of anillin on the stability of the contractile ring may be similar to the effect of microtubule-associated proteins to the dynamic stability of the mitotic spindle (39). It is likely that as cytokinesis progresses, the extent of the mechanical force exerted on the contractile ring increases. In the absence of anillin, the contractile ring is less stable and fails to withstand the mechanical force when cytokinesis progresses to a certain point, leading to the collapse of the cleavage furrow structure and the redistribution of active myosin.

Online Supplemental Materials—Time-lapse movies of HeLa cells are available in the Supplemental Materials. Cells were transfected with pSUPER (Movie 1) or pSUPER-anillin (Movies 2–5) and imaged every 15 s starting from 30 h after transfection. DIC images were shown in Movies 1 and 2. In Movies 3–5, HeLa cells stably expressing GFP-histone 2B were used, and images merged between DIC and green fluorescence channel were shown. In these movies, nocodazole (Movie 3), cytochalasin B (Movie 4), or blebbistatin (Movie 5) were added at the indicated concentrations as soon as the oscillatory movement began.

Acknowledgments—We thank Dr. Ryoko Kuriyama for the anti-CHO1 antibody, Akiko Seki for purifying the anti-MgcRacGAP antibody, and members of the Fang laboratory for discussions.

REFERENCES

1. Harper, J. W., Burton, J. L., and Solomon, M. J. (2002) *Genes Dev.* **16,** 2179–2206
2. Peters, J. M. (2002) *Mol. Cell* **9,** 931–943
3. Petersen, B. O., Wagener, C., Marinoni, F., Kramer, E. R., Melixetian, M., Denchi, E. L., Gieffers, C., Matteucci, C., Peters, J. M., and Helin, K. (2000) *Genes Dev.* **14,** 2330–2343
4. Li, A., and Blow, J. J. (2005) *EMBO J.* **24,** 395–404
5. McGarry, T. J., and Kirschner, M. W. (1998) *Cell* **93,** 1043–1053
6. Kramer, E. R., Gieffers, C., Holzl, G., Hengstschlager, M., and Peters, J. M. (1998) *Curr. Biol.* **8,** 1207–1210
7. Fang, G., Yu, H., and Kirschner, M. W. (1998) *Mol. Cell* **2,** 163–171
8. Pfleger, C. M., and Kirschner, M. W. (2000) *Genes Dev.* **14,** 655–665
9. Glotzer, M., Murray, A. W., and Kirschner, M. W. (1991) *Nature* **349,** 132–138
10. Echard, A., and O'Farrell, P. H. (2003) *Curr. Biol.* **13,** 373–383
11. Straight, A. F., Cheung, A., Limouze, J., Chen, I., Westwood, N. J., Sellers, J. R., and Mitchison, T. J. (2003) *Science* **299,** 1743–1747
12. Lustig, K. D., Stukenberg, P. T., McGarry, T. J., King, R. W., Cryns, V. L., Mead, P. E., Zon, L. I., Yuan, J., and Kirschner, M. W. (1997) *Methods Enzymol.* **283,** 83–99
13. Field, C. M., and Alberts, B. M. (1995) *J. Cell Biol.* **131,** 165–178
14. Oegema, K., Savoian, M. S., Mitchison, T. J., and Field, C. M. (2000) *J. Cell Biol.* **150,** 539–552
15. Echard, A., Hickson, G. R., Foley, E., and O'Farrell, P. H. (2004) *Curr. Biol.* **14,** 1685–1693
16. Somma, M. P., Fasulo, B., Cenci, G., Cundari, E., and Gatti, M. (2002) *Mol. Biol. Cell* **13,** 2448–2460
17. Straight, A. F., Field, C. M., and Mitchison, T. J. (2005) *Mol. Biol. Cell* **16,** 193–201
18. Paddison, P. J., Caudy, A. A., Bernstein, E., Hannon, G. J., and Conklin, D. S. (2002) *Genes Dev.* **16,** 948–958
19. Yu, J. Y., DeRuiter, S. L., and Turner, D. L. (2002) *Proc. Natl. Acad. Sci. U. S. A.* **99,** 6047–6052
20. Brummelkamp, T. R., Bernards, R., and Agami, R. (2002) *Science* **296,** 550–553
21. Hayashi, K., Yonemura, S., Matsui, T., and Tsukita, S. (1999) *J. Cell Sci.* **112,** 1149–1158
22. Charles, J. F., Jaspersen, S. L., Tinker-Kulberg, R. L., Hwang, L., Szidon, A., and Morgan, D. O. (1998) *Curr. Biol.* **8,** 497–507
23. Shirayama, M., Zachariae, W., Ciosk, R., and Nasmyth, K. (1998) *EMBO J.* **17,** 1336–1349
24. Pfleger, C. M., Lee, E., and Kirschner, M. W. (2001) *Genes Dev.* **15,** 2396–2407
25. De Lozanne, A., and Spudich, J. A. (1987) *Science* **236,** 1086–1091
26. Komatsu, S., Yano, T., Shibata, M., Tuft, R. A., and Ikebe, M. (2000) *J. Biol. Chem.* **275,** 34512–34520
27. Yamakita, Y., Yamashiro, S., and Matsumura, F. (1994) *J. Cell Biol.* **124,** 129–137
28. Eda, M., Yonemura, S., Kato, T., Watanabe, N., Ishizaki, T., Madaule, P., and Narumiya, S. (2001) *J. Cell Sci.* **114,** 3273–3284
29. Kosako, H., Yoshida, T., Matsumura, F., Ishizaki, T., Narumiya, S., and Inagaki, M. (2000) *Oncogene* **19,** 6059–6064
30. Glotzer, M. (2001) *Annu. Rev. Cell Dev. Biol.* **17,** 351–386
31. Lee, K. S., Yuan, Y. L., Kuriyama, R., and Erikson, R. L. (1995) *Mol. Cell. Biol.* **15,** 7143–7151
32. Liu, X., Zhou, T., Kuriyama, R., and Erikson, R. L. (2004) *J. Cell Sci.* **117,** 3233–3246
33. Hirose, K., Kawashima, T., Iwamoto, I., Nosaka, T., and Kitamura, T. (2001) *J. Biol. Chem.* **276,** 5821–5828
34. Tatsumoto, T., Xie, X., Blumenthal, R., Okamoto, I., and Miki, T. (1999) *J. Cell Biol.* **147,** 921–928
35. Terada, Y., Tatsuka, M., Suzuki, F., Yasuda, Y., Fujita, S., and Otsu, M. (1998) *EMBO J.* **17,** 667–676
36. Tasto, J. J., Morrell, J. L., and Gould, K. L. (2003) *J. Cell Biol.* **160,** 1093–1103
37. Bettinger, B. T., Gilbert, D. M., and Amberg, D. C. (2004) *Nat Rev Mol. Cell. Biol.* **5,** 410–415
38. Yoshizaki, H., Ohba, Y., Kurokawa, K., Itoh, R. E., Nakamura, T., Mochizuki, N., Nagashima, K., and Matsuda, M. (2003) *J. Cell Biol.* **162,** 223–232
39. Gadde, S., and Heald, R. (2004) *Curr. Biol.* **14,** R797–R805